Performance Investigation and Observer-based Condition Monitoring Scheme for a PMSG-based Grid-Connected Wind Power System under Switch Open Fault

Kyeong-Hwa Kim

Department of Electrical and Information Engineering
Seoul National University of Science and Technology
232 Gongneung-ro, Nowon-gu, Seoul, 139-743, Korea

k2h1@seoultech.ac.kr

Abstract

To analyze responses under open fault conditions in switching devices, a performance investigation and condition monitoring scheme are presented through an integrated simulation study of a permanent magnet synchronous generator (PMSG) based variable-speed grid-connected wind power system. Among various faults in power electronics components, the open fault in switching devices may arise due to the destruction of switches by an accidental over current or the forced disconnection for protection. When the switch open fault occurs in the generator-side converter, the grid-side inverter as well as the generator-side converter does not operate normally, resulting in an increase of the current harmonics and a reduction in generated output and efficiency. As an effective way of the condition monitoring for the generation system by online basis without requiring any diagnostic apparatus, the estimation schemes for the generated voltage, flux linkage, and stator resistance are proposed in this paper and the validity of the proposed scheme is proved through comparative simulations.

Keywords: *Condition monitoring, Grid-connected, PMSG, Switch open fault, Wind power*

1. Introduction

Over the last ten years, there has been an increasing interest in the renewable energy sources because of the worldwide energy crisis created by the depletion of fossil energy and the greenhouse gas emission limit. Among various renewable energy resources connected to the grid, wind power generation is recognized as the most competitive and economic one, which leads to a rapid growth in the global wind power generation capacity [1-3].

While the early technology in a wind turbine is based on constant-speed squirrel-cage induction generator (SCIG) directly connected to the grid, a variable-speed technology with high efficiency and reduced mechanical stress has been developed recently. In the variable-speed drive, a back-to-back converter composed of a three-phase converter and a grid-connected inverter is located between the generator and grid, which converts the generator output in variable voltage and variable frequency to the fixed voltage and frequency of the grid [1]. A permanent magnet synchronous generator (PMSG) using the back-to-back converter for a variable-speed wind power generation has the advantages of simple structure, high efficiency, wide operating range, and no loss in field winding. In addition, PM excitation allows generators to have a smaller pole pitch as compared with the conventional ones, which makes it possible to design a generator at rated speeds of 20–200 rpm by adopting multiple pole configurations [4]. This eliminates the need for the gearbox which is the main cause of

noise and decrease in reliability, and permits a direct drive mechanism coupled to the grid. Thus, many researchers have been focusing on PMSG-based variable-speed grid-connected wind power generation systems. Recent studies on wind power generation systems aim to combine power converters with the control theory in the fields of a maximum power point tracking (MPPT), a pitch control, a grid connection, and a compliant operation with the grid code [5].

Whereas a stand-alone wind power generation was often used or small wind power was connected to the grid in the past, the level of wind energy penetration in the electrical power systems has been increased recently because the wind power equipment is being produced on much larger scale. Therefore, the issue of improving the stability in the utility grid operation through the improvement of the reliability and efficiency in the wind power generation system has become a major concern. For this purpose, an advanced maintenance scheme based on a fault diagnosis and condition monitoring has been reported for the next-generation wind power generation system [6-8]. Considering that the recent large-scale wind power systems have been built in off shore or remote locations, leading to considerable times and costs for maintenance or repair, this issue will become more important.

In general, the fault diagnosis and remedial strategy can be dealt with according to five procedures, these are, the condition monitoring, fault diagnosis, fault-tolerant operation, fault prediction, and fault avoidance. In early stage of a certain fault, the system may still operate. If left undetected, however, such a fault may easily be propagated to adjacent system, leading to another fault. To minimize the repair cost by detecting the fault at the initial stage, the correct condition monitoring and fault diagnosis scheme play a more important role. Recently, the analytic result for the average fault rate in a wind power generation system has been presented in detail [9]. According to this work, the bearing, generator, rotor eccentricity, and electrical components are the main cause of the fault. Among the faults in electrical components, 50% of the faults occur in the power converter such as back-to-back converters, and the other 50% in the remaining components. The faults in electrical components are increasing steadily as the use of full power converters grows.

Recently, to realize a fault-tolerant operation, a modular power electronic converter has been proposed as the grid interface of a large direct-drive wind turbine generator. In this work, each converter module is connected to isolated generator coils to provide a tolerance to a module converter or generator coil [10]. A condition monitoring system based on sensor networks using a vibrating sensor or an acceleration sensor has been developed [6]. Even though such a system mainly focuses on the condition monitoring for the drive train parameters such as the turbine mass imbalance, shaft defect, and bearing damage, a diagnosis and remedial strategy for internal faults in the generator and the power electronic converter are not sufficient.

While fault diagnosis schemes for a PMSG or inverter as a single unit have been studied partly [11-14], those under the direct connection to the wind turbine are not sufficient. Thus, on-line basis fault diagnosis schemes that the controller can detect a fault during the operation without any additional diagnostic equipment such as sensor networks are much required for the wind power generation system. Since variable-speed wind turbines often undergo a severe mechanical and environmental stress, a minor fault may be continuously propagated and magnified to adjacent system. Whereas considerable costs are required to restore the system in an extreme situation, the loss for rehabilitation can be minimized if a fault is detected at an initial stage of failure.

In this paper, a performance investigation and condition monitoring scheme for a PMSG-based variable-speed grid-connected wind power system are presented through an integrated simulation research when an open fault occurs in switching devices. Among

various cause of faults in power electronic converters, the failure in switching devices is due to the damage caused by over-current or the forced disconnection by protection circuits. If the fault in the switching devices occurs in the generator-side converter, the three-phase voltages calculated in the controller cannot be synthesized accurately in the converter, which increases harmonic components in current and decreases the generated power. To detect such faults and monitor the normal operation of system, three types of observer schemes for parameters are proposed, where the no-load generated voltage, flux linkage, and stator resistance of the PMSG are estimated using the observer or adaptive control methods. To verify that monitoring these parameters are effective to detect the open fault in the switching devices of the power electronic converter, integrated simulation results are presented.

2. Modeling of Wind Power Generation System

The overall configuration for the wind power generation system employing a back-to-back converter and PMSG is shown in Figure 1. The kinetic energy of the wind produces a mechanical torque with the blade of a wind turbine, which is converted into the electric energy through the PMSG and back-to-back converter and then supplied to the grid. The generator-side converter controls the speed of the generator to draw the maximum output power from the wind turbine and the grid-side inverter controls the frequency and active/reactive powers for the grid connection.

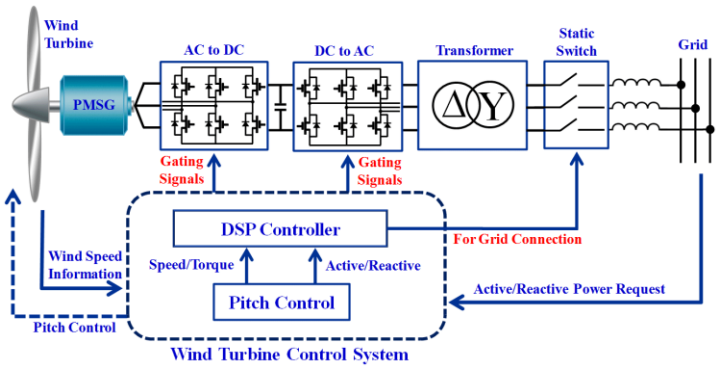

Figure 1. Configuration of the grid-connected wind power generation system

The blade is used for converting the kinetic energy of the wind to the mechanical rotational energy. When the wind with velocity V_{wind} [m/s] passes through the wind turbine with a rotor radius R_b [m], the wind power is expressed as

$$P_{wind} = 0.5A\rho V_{wind}^3 \ [W] \quad (1)$$

where $A = \pi R_b^2$ is the cross sectional area of the rotor blade [m^2] and ρ is the air density [kg/m^3]. The power converted by a wind turbine from P_{wind} can be expressed as

$$P_b = 0.5A\rho V_{wind}^3 C_p(\lambda,\beta) \ [W] \quad (2)$$

where C_p is the power coefficient of the turbine, β is the pitch angle, and λ is the tip speed ratio (TSR). The power coefficient C_p is usually given as a function of the λ as well as β. The TSR λ is given by

$$\lambda = \omega_b R_b / V_{wind} \quad (3)$$

where ω_b is the rotational angular speed of the wind turbine. The power coefficient C_p represents the power conversion efficiency of the wind turbine and is expressed as follows [15]:

$$C_p = c_1 \cdot (c_2 - c_3\beta - c_4\beta^x - c_5) \cdot e^{-c_6}. \quad (4)$$

In general, the power coefficient C_p has a maximum value of $C_{p\max}$ when the TSR λ is maintained at λ_{opt}. When the power coefficient is $C_{p\max}$, the power captured by the wind turbine becomes maximum and expressed as

$$P_{b\max} = 0.5A\rho C_{p\max} V_{wind}^3 = 0.5A\rho C_{p\max} (\omega_b R_b / \lambda)^3. \quad (5)$$

The power captured by the wind turbine is delivered to a PMSG as a torque and the torque T_b delivered to the PMSG can be expressed as $T_b = P_b / \omega_b$.

3. PMSG-based variable-speed grid-connected Wind Power Systems

In the synchronous reference frame, the stator voltage equations of the PMSG are expressed as follows [16]:

$$e_{qem} = (R_s + pL_q) i_{qem} + \omega_r L_d i_{dem} + v_{qem} \quad (6)$$

$$e_{dem} = (R_s + pL_d) i_{dem} - \omega_r L_q i_{qem} + v_{dem} \quad (7)$$

where subscript "m" denotes the variables in the generator and generator-side converter, v_{qem} and v_{dem} are the *q*-axis and *d*-axis stator voltages, respectively, i_{qem} and i_{dem} are the *q*-axis and *d*-axis stator currents, respectively, R_s is the stator resistance, L_q and L_d are the *q*-axis and *d*-axis inductances, respectively, ω_r is the electrical angular velocity of the generator, and p is a differential operator. If the generated voltage is aligned to the *q*-axis in the synchronous reference frame, $e_{qem} = \omega_r \lambda_m$ and $e_{dem} = 0$ where λ_m represents the flux linkage established by the permanent magnet. When the increasing ratio of the gear is N, the torque delivered to the PMSG by the wind turbine is $T_m = T_b / N$, and the electromagnetic torque of the PMSG is represented as

$$T_m = J p\omega_m + B\omega_m + T_e \quad (8)$$

$$T_e = 1.5 n_p [(L_d - L_q) i_{dem} i_{qem} + \lambda_m i_{qem}] \quad (9)$$

where J is the total equivalent inertia of the wind turbine and generator, B is the friction coefficient, n_p is the number of the generator pole pairs, ω_m is the mechanical angular velocity of the generator expressed as $\omega_m = N\omega_b = \omega_r / n_p$.

For a given wind speed and pitch angle, there is an optimal TSR λ_{opt} under which C_p is maximum. For the maximum power extraction from the wind, the generator-side converter is controlled in order to ensure that TSR is maintained at λ_{opt}, and thus, C_p becomes $C_{p\max}$ [1]. When TSR is controlled to λ_{opt}, the maximum mechanical power and torque delivered to the PMSG are obtained from (5) as follows:

$$P_{b\max} = K_b \omega_b^3 \tag{10}$$

$$T_{b\max} = K_b \omega_b^2 \tag{11}$$

where $K_b = 0.5A\rho C_{p\max}(R_b / \lambda_{opt})^3$. From (11), the q-axis current reference of the PMSG can be determined as

$$i_{qem}^* = T_{m\max} / K_t = T_{b\max} / (NK_t) \tag{12}$$

where the symbol "*" denotes the reference quantity and $K_t = 1.5 n_p \lambda_m$ is the torque constant of the PMSG. The speed and torque controls of the PMSG are achieved through a current control of the generator-side converter. The current controller is accomplished on the synchronous reference frame using the q-axis current reference in (12) and the d-axis current reference $i_{dem}^* = 0$ for unity power factor. With the PI decoupling control, the voltage references are calculated as follows:

$$v_{qem}^* = -(k_{pm} + k_{im} / s)(i_{qem}^* - i_{qem}) - \omega_r L_d i_{dem} + e_{qem} \tag{13}$$

$$v_{dem}^* = -(k_{pm} + k_{im} / s)(i_{dem}^* - i_{dem}) - \omega_r L_q i_{qem} \tag{14}$$

where k_{pm} and k_{im} represent the proportional and integral gains, respectively, and s is the Laplace operator. In the generator-side converter, the q-axis and d-axis components of the current control the generator torque and power factor, respectively, and the computed voltage references are applied with the space vector PWM technique [17].

In a variable-speed wind power generation system using the back-to-back converter, the grid-side inverter delivers the generated power to the grid with unity power factor by controlling the inverter output current in phase with the grid voltage. When the input power to the DC link becomes larger than the output power to grid, the DC link voltage is increased, and in the opposite case, the DC link voltage is decreased. By controlling the DC link voltage constantly, the grid-side inverter can deliver the power from the generator-side converter to the grid [3]. The active and reactive powers to the grid are determined as

$$P = 1.5(e_{qeg} i_{qeg} + e_{deg} i_{deg}) \tag{15}$$

$$Q = 1.5(e_{qeg} i_{deg} - e_{deg} i_{qeg}) \quad (16)$$

where subscript "g" represents the variables in the grid and grid-side inverter, e_{qeg} and e_{deg} are the *q*-axis and *d*-axis grid voltages, respectively, and i_{qeg} and i_{deg} are the *q*-axis and *d*-axis currents, respectively. Since i_{deg} is normally controlled to zero for the reactive power of zero, the active power becomes $P = 1.5Ei_{qeg}$ with $e_{qeg} = E$ and $e_{deg} = 0$. The grid-side inverter consists of an outer-loop voltage controller to control the DC link voltage and an inner-loop current controller. Using the PI control, the voltage controller can be expressed as

$$i^*_{qeg} = -(k_{pv} + k_{iv} / s)(V^*_{DC} - V_{DC}) \quad (17)$$

where V_{DC} is the DC link voltage. With (17) and the current reference of $i^*_{deg} = 0$, the current controller is achieved using the PI decoupling control on the synchronous reference frame as follows:

$$v^*_{qeg} = (k_{pg} + k_{ig} / s)(i^*_{qeg} - i_{qeg}) + \omega_e L_s i_{deg} + e_{qeg} \quad (18)$$

$$v^*_{deg} = (k_{pg} + k_{ig} / s)(i^*_{deg} - i_{deg}) - \omega_e L_s i_{qeg} + e_{deg} \quad (19)$$

where ω_e is the angular velocity of the grid voltage.

4. Fault Model and Condition Monitoring of PMSG-based Variable-speed Wind Power Systems

When an open fault occurs in switching devices, it is difficult to obtain the converter input voltage with the phase voltage model or the conventional *dq* model since three-phase balanced condition does not hold. Therefore, to analyze influences under such a fault condition, a model based on the line-to-line voltage has to be used. Figure 2 shows the PMSG and three-phase PWM converter. The pole voltages v_{ao}, v_{bo}, and v_{co} are defined as the terminal voltages of the PMSG with respect to DC link ground "o" of converter. The *a*-phase pole voltage is determined according to the conduction state of switch or diode as

$v_{ao} = V_{DC}$ for T_{a+} or D_{a+} on

$v_{ao} = 0$ for T_{a-} or D_{a-} on

The phase voltages v_{asm}, v_{bsm}, and v_{csm} are defined as the terminal voltages with respect to the neutral point "s" of the PMSG. The relation for the line voltage, phase voltage, and pole voltage are expressed as follows:

$$v_{ab} = v_{asm} - v_{bsm} = v_{ao} - v_{bo} \quad (20)$$

$$v_{bc} = v_{bsm} - v_{csm} = v_{bo} - v_{co} \quad (21)$$

$$v_{ca} = v_{csm} - v_{asm} = v_{co} - v_{ao} \tag{22}$$

Since three-phase balanced condition holds under the normal operating condition, the phase voltages of the PMSG can be easily obtained from the pole voltages according to switching states. However, it does not hold any longer under the open fault in switching devices, making it difficult to obtain the phase voltage inputs of the PMSG. Thus, to obtain a fault model that can be simply used for the simulation, line-to line voltages should be used. Using (20)-(22), the PMSG model under the normal operating condition without a fault can be expressed as follows [16]:

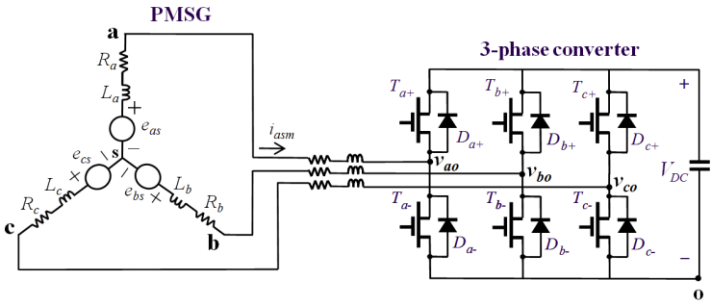

Figure 2. PMSG and three-phase PWM converter

$$-p(L-M)i_{asm} + p(L-M)i_{bsm} = v_{ab} - e_{asm} + e_{bsm} + R_s i_{asm} - R_s i_{bsm} \tag{23}$$

$$-p(L-M)i_{asm} - 2p(L-M)i_{bsm} = v_{bc} - e_{bsm} + e_{csm} + R_s i_{asm} + 2R_s i_{bsm}. \tag{24}$$

where R_s is the stator resistance, L is the self inductance, M is the mutual inductance, i_{asm}, i_{bsm}, and i_{csm} are the phase currents, respectively, e_{asm}, e_{bsm}, and e_{csm} are the three-phase generated voltages of the PMSG.

To derive a fault model caused by the failure in the three-phase converter of a wind power system, the case that both the switches in one converter leg have the open fault is considered first. When the open fault arises in T_{a+} and T_{a-} in Figure 2 at the same time, *a*-phase winding of the generator is completely separated from the converter and cannot supply power to the DC link. This fault may arise when the entire switch is destructed by an accidental over current, or a fuse connected for short protection is blown out. In this case, *a*-phase current is maintained to zero, and the generated power is delivered to the DC link only through the other two phases. In three-phase Y-connection with $i_{asm} = 0$, $i_{bsm} + i_{csm} = 0$ and $i_{bsm} = -i_{csm}$ are obtained. Furthermore, $v_{asm} = e_{asm}$ is given. Since the phase current having open fault is kept to zero, the differential equation can be established by using the other two phases. While the order of the state equations is two under the normal condition, it is reduced to one under this condition. From the phase voltage v_{bsm} and v_{csm}, the line-to-line voltage model under the open fault in T_{a+} and T_{a-} is obtained as

$$v_{bc} = -2p(L-M)i_{bsm} - 2R_s i_{bsm} + e_{bsm} - e_{csm} \tag{25}$$

With (25), the fault model and response characteristics can be obtained when the open fault occurs in the entire arm switch in *a*-phase. Table 1 shows the voltage model when the open fault arises in the entire switch of one leg in the three-phase converter.

Next, the case when one out of six switches in the three-phase converter of Figure 2 has the open fault is considered. Figure 3 shows the switching pattern in the symmetrical space vector PWM. When the open fault arises in *a*-phase upper switch T_{a+}, it is impossible to produce the voltage vectors $\boldsymbol{V_1}$, $\boldsymbol{V_3}$, $\boldsymbol{V_5}$, and $\boldsymbol{V_7}$ in Figure 3 exactly because they need the conduction of T_{a+}. Since such active vectors have to be used in sectors 1, 2, 5, and 6, the converter cannot synthesize the average voltages equal to reference in these sectors. Although sectors 3 and 4 do not require the conduction of T_{a+}, the zero vector $\boldsymbol{V_7}$ as shown in Figure 3 cannot be generated. In case of the open fault only in T_{a+}, the pole voltage v_{ao} is explicitly determined as $v_{ao}=0$ due to the conduction of T_{a-} in the vectors $\boldsymbol{V_0}$, $\boldsymbol{V_2}$, $\boldsymbol{V_4}$ and $\boldsymbol{V_6}$. In the vectors $\boldsymbol{V_1}$, $\boldsymbol{V_3}$, $\boldsymbol{V_5}$, and $\boldsymbol{V_7}$, however, v_{ao} has an instantaneous transient voltage caused by v_{bo}, v_{bsm}, and v_{asm}, and becomes zero at steady-state.

Table 1. Voltage model under the open fault in entire switch of one converter arm

Faulty phase	Voltage model
a-phase	$i_{asm}=0,\ v_{asm}=e_{asm},\ i_{bsm}+i_{csm}=0,\ \dot{i}_{bsm}=-\dot{i}_{csm}$ $v_{bc}=-2p(L-M)i_{bsm}-2R_s i_{bsm}+e_{bsm}-e_{csm}$
b-phase	$i_{bsm}=0,\ v_{bsm}=e_{bsm},\ i_{asm}+i_{csm}=0,\ \dot{i}_{asm}=-\dot{i}_{csm}$ $v_{ca}=-2p(L-M)i_{csm}-2R_s i_{csm}+e_{csm}-e_{asm}$
c-phase	$i_{csm}=0,\ v_{csm}=e_{csm},\ i_{asm}+i_{bsm}=0,\ \dot{i}_{asm}=-\dot{i}_{bsm}$ $v_{ab}=-2p(L-M)i_{asm}-2R_s i_{asm}+e_{asm}-e_{bsm}$

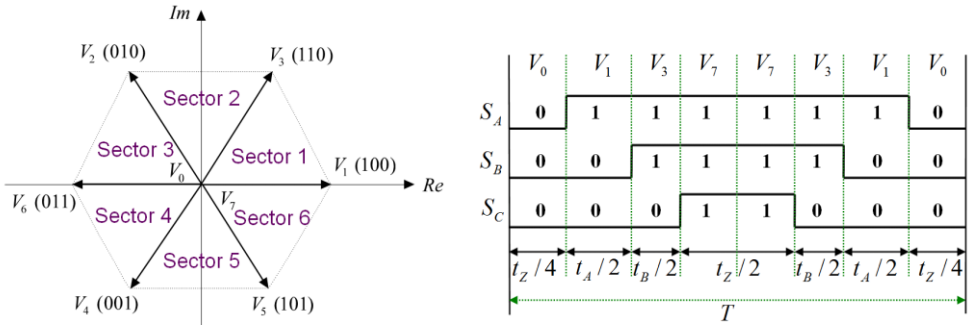

Figure 3. Switching pattern in the symmetrical space vector PWM

When the switch open fault happens in the three-phase converter in a variable-speed wind power system based on the PMSG and back-to-back converter, it will not be able to control TSR in order to maintain the power coefficient of the turbine at the maximum. As a result, the maximum generated power as well as unity power factor cannot be obtained through current control. Thus, an exact fault detecting or condition

monitoring technique that can detect a failure in the generation system is demanded to improve the reliability and efficiency.

In this paper, three parameter observation schemes that can detect a switch open fault in the three-phase converter as well as monitor a normal operation is proposed. Considering that the three-phase converter is often operated with the PMSG, the no-load generated voltage, flux linkage, and stator resistance of the PMSG are estimated through the observer or adaptation schemes. It is proved that monitoring these parameters can be effectively used to detect a switch open fault in three-phase converter.

The q-axis no-load generated voltage of the PMSG $e_{qem} = \omega_r \lambda_m$ is estimated using a disturbance observer theory. Although e_{qem} in (6) is not a state variable, the conventional observer can be easily extended to estimate e_{qem}. With the assumption that the observer has much faster dynamics than the time variation of e_{qem}, $\dot{e}_{qem} = 0$ holds during each sampling intervals of current control [18]. Using this assumption and (6), the state equation can be obtained as follows:

$$p\begin{pmatrix} i_{qem} \\ e_{qem} \end{pmatrix} = \begin{pmatrix} -R_s / L_q & 1/L_q \\ 0 & 0 \end{pmatrix} \cdot \begin{pmatrix} i_{qem} \\ e_{qem} \end{pmatrix} - \begin{pmatrix} 1/L_q \\ 0 \end{pmatrix} v_{qem} + \begin{pmatrix} -\omega_r (L_d / L_q) i_{dem} \\ 0 \end{pmatrix}. \quad \textbf{(26)}$$

Because this system is observable, full states in (26) can be completely observed. To reduce the computational load, a reduced-order observer can be used to estimate $\hat{e}_{qem}$.

As another method of a condition monitoring or detection for the switch open fault, the estimation of flux linkage can be used. Similarly, when the disturbance observer has sufficiently faster dynamics than the time variation of λ_m, $\dot{\lambda}_m = 0$ also holds during each sampling intervals. From $e_{qem} = \omega_r \lambda_m$ and (6), the state equation is given as

$$p\begin{pmatrix} i_{qem} \\ \lambda_m \end{pmatrix} = \begin{pmatrix} -R_s / L_q & \omega_r / L_q \\ 0 & 0 \end{pmatrix} \cdot \begin{pmatrix} i_{qem} \\ \lambda_m \end{pmatrix} - \begin{pmatrix} 1/L_q \\ 0 \end{pmatrix} v_{qem} + \begin{pmatrix} -\omega_r (L_d / L_q) i_{dem} \\ 0 \end{pmatrix}. \quad \textbf{(27)}$$

Since (27) is completely observable, the estimate of flux linkage $\hat{\lambda}_m$ can be obtained through a reduced-order observer.

For the failure detection and condition monitoring in the three-phase converter, the stator resistance of the PMSG can be used. The stator resistance is estimated using the hyperstability concept of the model reference adaptive control (MRAC) scheme [19]. From (6) and (7), the state equation can be obtained as follows:

$$p\boldsymbol{i_s} = \boldsymbol{A i_s} + \boldsymbol{B v_s} + \boldsymbol{d}$$

$$p\begin{pmatrix} i_{qem} \\ i_{dem} \end{pmatrix} = \begin{pmatrix} -R_s / L_q & -\omega_r L_d / L_q \\ \omega_r L_q / L_d & -R_s / L_d \end{pmatrix} \begin{pmatrix} i_{qem} \\ i_{dem} \end{pmatrix} + \begin{pmatrix} -1/L_q & 0 \\ 0 & -1/L_d \end{pmatrix} \begin{pmatrix} v_{qem} \\ v_{dem} \end{pmatrix} + \begin{pmatrix} e_{qem} / L_q \\ e_{dem} / L_d \end{pmatrix} \quad \textbf{(28)}$$

The full-order observer which estimates the full states in (28) is expressed as

$$p\hat{\boldsymbol{i}}_{\boldsymbol{s}} = \hat{\boldsymbol{A}}\hat{\boldsymbol{i}}_{\boldsymbol{s}} + \boldsymbol{B v_s} + \boldsymbol{d} + \boldsymbol{G}(\hat{\boldsymbol{i}}_{\boldsymbol{s}} - \boldsymbol{i_s}). \quad \textbf{(29)}$$

where $\hat{A} = \begin{pmatrix} -\hat{R}_s / L_q & -\omega_r L_d / L_q \\ \omega_r L_q / L_d & -\hat{R}_s / L_d \end{pmatrix}$, $G = \begin{pmatrix} g_{11} & g_{12} \\ g_{21} & g_{22} \end{pmatrix}$

and "$\wedge$" denotes the estimated quantities. If the error between the current and its estimate is defined as $\boldsymbol{e} = \boldsymbol{i_s} - \hat{\boldsymbol{i}}_s$, the error dynamic equation can be obtained by subtracting (29) from (28) as follows:

$$\dot{\boldsymbol{e}} = (\boldsymbol{A} + \boldsymbol{G})\boldsymbol{e} - \boldsymbol{W} \tag{30}$$

where $\boldsymbol{W} = -(\boldsymbol{A} - \hat{\boldsymbol{A}})\hat{\boldsymbol{i}}_s = -\Delta R_s \boldsymbol{B}\hat{\boldsymbol{i}}_s$ and $\Delta R_s = R_s - \hat{R}_s$. From (30), the adaptation mechanism can be defined as

$$\hat{R}_s(e,t) = \int_0^t \Phi_1 d\tau + \Phi_2 + \hat{R}_s(0) \tag{31}$$

where Φ_1 and Φ_2 are the adaptation mechanisms for R_s estimation and $\hat{R}_s(0)$ denotes the initial estimate. A design problem for an adaptive control for the asymptotic stability is summarized as [19]

1. Determine Φ_1 and Φ_2 to ensure $\lim_{t\to\infty} \boldsymbol{e}(t) = 0$ for initial conditions $\boldsymbol{e}(0)$ and $\Delta R_s(0)$
2. Find the adaptation rule which lead to $\lim_{t\to\infty} \hat{R}_s = R_s$.

This system is asymptotically stable if the matrix $(\boldsymbol{A} + \boldsymbol{G})$ is strictly positive real and $\boldsymbol{W}$ satisfies the Popov's integral inequalities. This is satisfied by selecting the adaptation mechanism of R_s as

$$\hat{R}_s = (k_{PR} + k_{IR}/s) \cdot (\boldsymbol{e}^T \boldsymbol{B}\hat{\boldsymbol{i}}_s) + \hat{R}_s(0) \tag{32}$$

where k_{PR} and k_{IR} are the proportional and integral gains for R_s estimation.

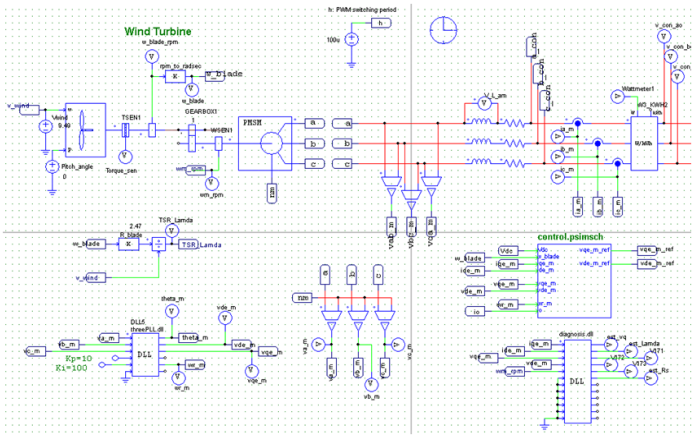

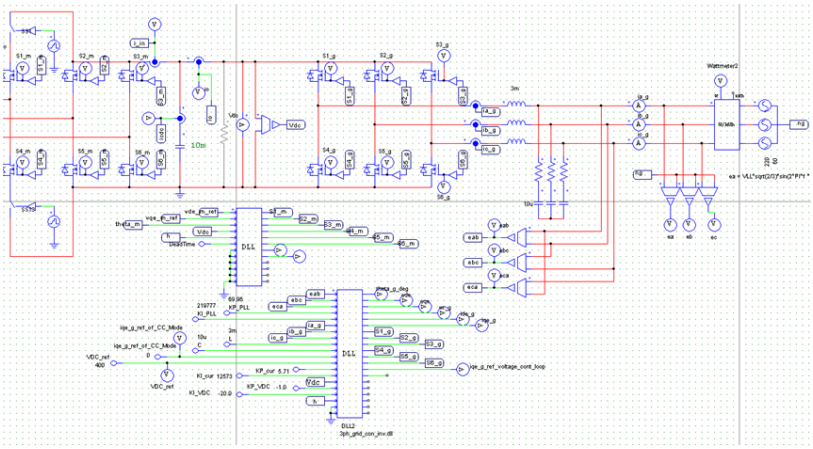

Figure 4. Simulation configuration of a PMSG-based wind power system

5. Simulation result

In this section, we analyze the response characteristics under the open fault in switching devices through the integrated simulation studies of the PMSG-based variable-speed grid-connected wind power system. In addition, it is proved by comparative simulations that the estimation of three parameters can be used effectively for a fault diagnosis and condition monitoring.

The entire simulation is done by using the PSIM software and the main controller is implemented with the PSIM DLL block. Figure 4 shows the integrated simulation structure for a PMSG-based variable speed grid-connected wind power system. The overall system consists of a wind turbine, a PMSG, a generator-side converter, a grid-side inverter, and DLL blocks for the controller implementation. For a current control in the converter and inverter, the synchronous frame PI decoupling control is used with the sampling period of 100 μsec. To apply the computed reference voltages to the generator-side converter as well as to the grid-side inverter, the symmetrical space vector PWM technique is employed. For a wind turbine model, the PSIM model block with $C_{p,\max}$ = 0.49 at λ_{opt} = 8.18 is used in the simulation. The simulation was performed using real parameter values except for the turbine inertia, which was set relatively low in order to reduce the calculation time and to observe the transient state. The parameters of the wind turbine and PMSG are listed in Table 2.

Table 2. Parameters of a wind turbine blade and PMSG

Wind turbine	Rated power	5 kW
	Rated wind speed	9.5 m/sec
	Rated speed	300 rpm
	Blade radius	2.5 m
PMSG	Rated power	5 kW
	Rated speed	300 rpm
	Number of poles	24
	Flux linkage	0.36 Wb
	Stator resistance	0.64 Ω
	Stator inductance	0.82 mH

Figure 5 shows the simulation results for the wind power generation system under the normal operating conditions. While the operation of the generator-side converter starts at $t=0$, the operation of the grid-side inverter does at 0.05 sec. The first figure in Figure 5 shows a-phase generator voltage v_{asm} and current i_{asm} in the generator-side converter. It is clearly shown that the phase current is close to sinusoidal and in phase with voltage to provide unity power factor. The second figure shows a-phase grid voltage e_{asg} and current i_{asg} controlled by the grid-side inverter. It is confirmed that the grid output current is sinusoidal and in phase with the grid voltage, which delivers the power to the grid with unity power factor. The third figure shows the DC link voltage reference V_{DC}^{*} and DC link voltage V_{DC}. To show that the current control is accomplished effectively, the fourth figure shows the q-axis current reference i_{qeg}^{*}, q-axis current i_{qeg}, d-axis current i_{deg}, and a-phase current i_{asg} in the grid-side inverter. The fifth through seventh figures show the input power W_{in} and output power W_{out} of the back-to-back converter, respectively, the torque T_m supplied to PMSG from the wind turbine, and TSR λ. It can be confirmed that the output power is 4 kW and the TSR is controlled to λ_{opt} of 8.18.

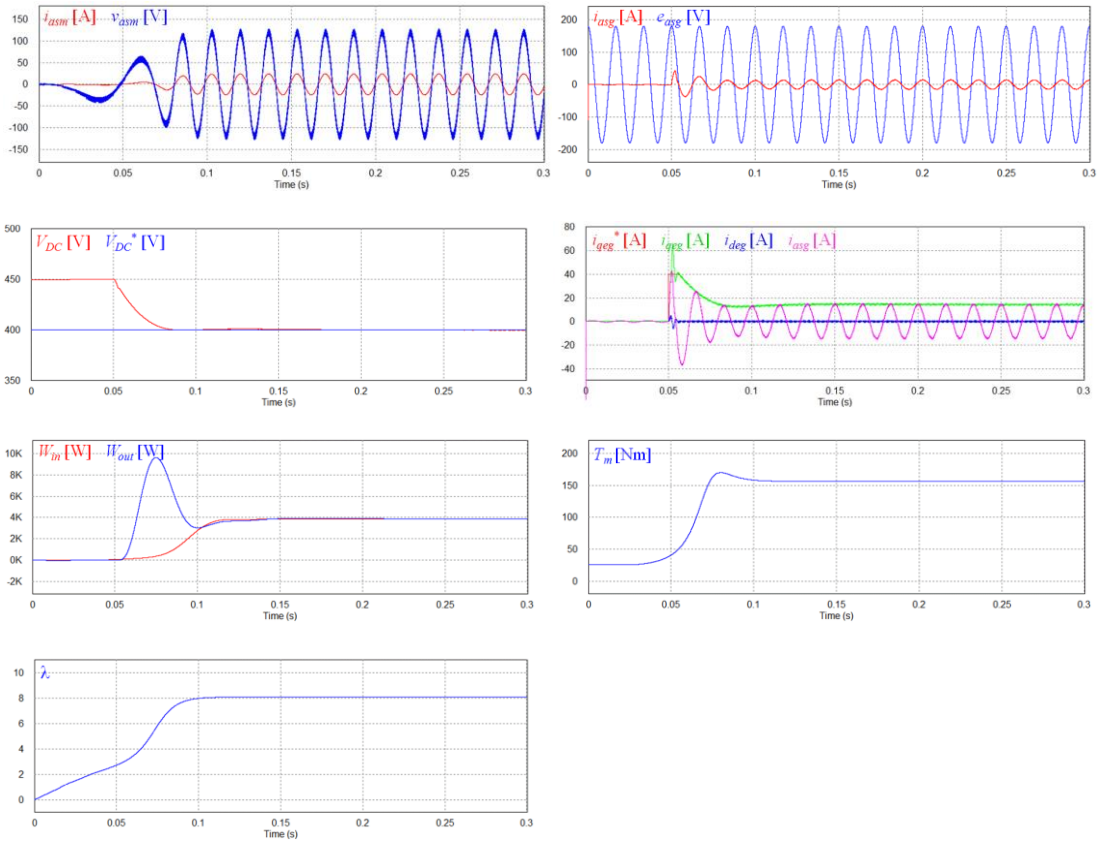

Figure 5. Simulation results under the normal operating conditions

Figure 6 shows the simulation results for the condition monitoring when *a*-phase upper switch T_{a+} in the generator-side three-phase converter has an open fault at 0.2 sec. The normal operation is changed to abnormally at 0.2 sec. In this case, only the positive *a*-phase current can flow from the generator to the three-phase converter. Three-phase currents cannot maintain balanced condition even under the open fault in one switch, and the other phase currents unrelated to the fault are not controlled. Also, *a*-phase generator voltage waveform is deteriorated, which affects the control quality in the DC link voltage. The DC link voltage control characteristics affect the control performance in the *q*-axis and *d*-axis current control of the grid-side inverter which is irrespective of fault. This eventually results in the decrease in power factor and grid output power. The estimation of the no-load generated voltage e_{qem}, flux linkage λ_m, and stator resistance R_s of the PMSG starts at 0.1 sec. Whereas the estimates of all the parameters reach the nominal values within 0.01 sec under the normal condition without a switch open fault, they show unusual vibrating characteristics as soon as the switch open fault occurs. From these results, it can be confirmed that monitoring theses parameters can be used effectively to detect an abnormal system operation.

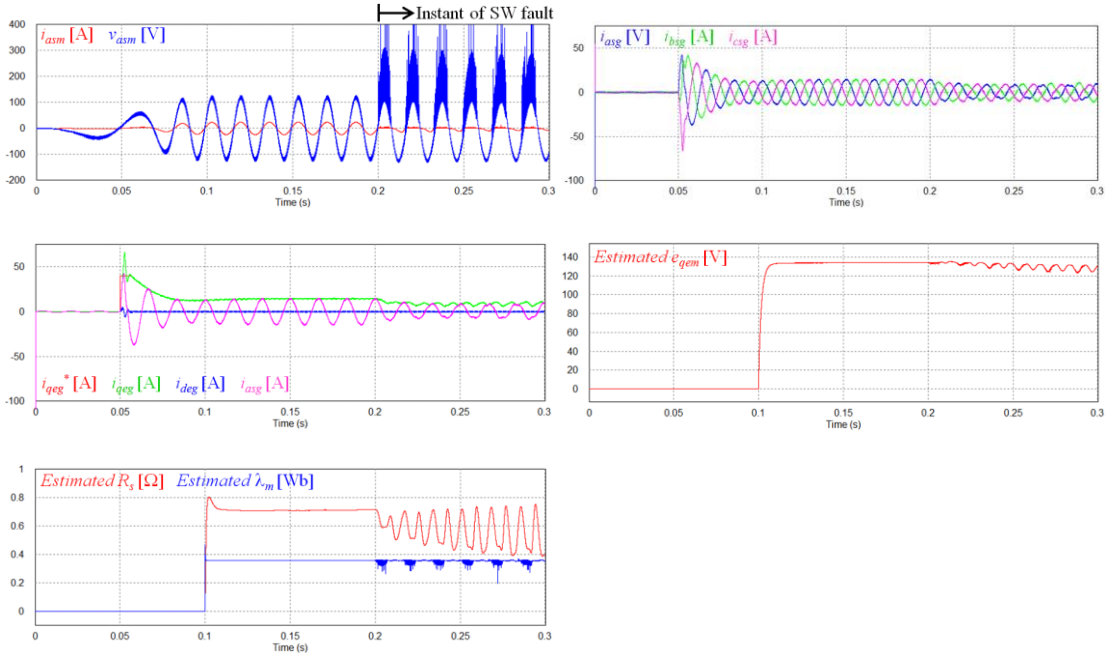

Figure 6. Simulation results and condition monitoring under T_{a+} switch open fault in the generator-side three-phase converter

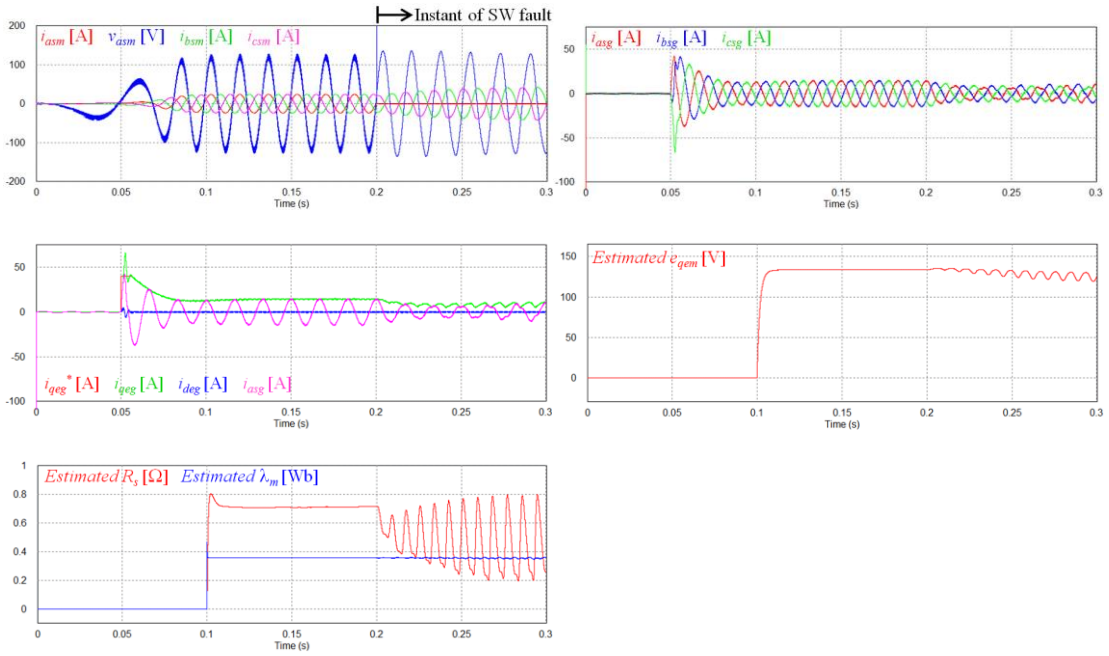

Figure 7. Simulation results and condition monitoring under the entire switch open fault in *a*-phase of the generator-side three-phase converter

Figure 7 shows the simulation results for the condition monitoring when an open fault occurs at 0.2 sec in entire *a*-phase switch of the generator-side three-phase converter. The system operation is changed abnormally from 0.2 sec. Even in the other phases unrelated to the fault, the PMSG and converter cannot be operated with unity power factor, which affects the control of the DC link voltage as well as grid-side inverter, eventually causing the performance degradation in the wind power generation. It can be seen that the estimated values of e_{qem}, λ_m, and R_s show an abnormal vibration under the open fault in the switch while they converge quickly to their actual values under the normal condition. From these results, it is confirmed that the active and reactive power control as well as the maximum power generation cannot be achieved in the presence of an open fault even in a single switch and the proposed condition monitoring schemes can be effectively used to detect an abnormal operation.

6. Conclusions

To analyze influences caused by the open fault in switching devices in a wind power generation system employing a back-to-back converter and PMSG, a fault model as well as a condition monitoring scheme useful for a performance assessment has been presented through an integrated simulation. Among the various cause of switch faults in power electronic converters, the open fault in one switch or entire switch in one converter leg on the generator-side converter was considered. This failure may arise due to the damage caused by over-current or the forced disconnection by protection circuits. If the open fault in the switching devices occurs in the generator-side converter, the three-phase voltage references calculated in the controller cannot be synthesized accurately in the converter, which causes an increase in the current harmonic components as well as the decrease in the generated power. This introduces the

increased harmonics in the grid-side inverter and reduced output power to the grid. In this paper, as an effective way to improve the reliability of the generation system and detect the faults in system with an online basis without any additional equipment, a monitoring scheme for three types of parameters has been proposed, where the no-load generated voltage, flux linkage, and stator resistance of the PMSG are estimated using the observer or adaptive control methods. The effectiveness of the proposed condition monitoring schemes has been verified through the integrated simulation research.

Acknowledgements

This research was supported by Basic Science Research Program through the National Research Foundation of Korea(NRF) funded by the Ministry of Education, Science and Technology (2012R1A1A2042759).

References

[1] Z. Chen, J. M. Guerrero and F. Blaabjerg, "A review of the state of the art of power electronics for wind turbines", IEEE Transactions on Power Electronics, vol. 24, no. 8, **(2009)**, pp. 1859-1875.
[2] I. Munteanu, S. Bacha, A. Bratcu, J. Guiraud and D. Roye, "Energy-reliability optimization of wind energy conversion systems by sliding mode control", IEEE Transactions on Energy Conversion, vol. 23, no. 3, **(2008)**, pp. 975-985.
[3] S. Grabic, N. Celanovic and V. Katic, "Permanent magnet synchronous generator cascade for wind turbine applications", IEEE Transactions on Power Electronics, vol. 23, no. 3, **(2008)**, pp. 1136-1142.
[4] A. D. Hansen and G. Michalke, "Multi-pole permanent magnet synchronous generator wind turbines' grid support capability in uninterrupted operation during grid faults", IET Renewable Power Generation, vol. 3, no. 3, **(2009)**, pp. 333-348.
[5] A. H. Kasem, E. F. El-Saadany, H. H. El-Tamaly and M. A. A. Wahab, "An improved fault ride-through strategy for doubly fed induction generator-based wind turbines", IET Renewable Power Generation, vol. 2, no. 4, **(2008)**, pp. 201-214.
[6] ISET Offshore M&R Final Public Report, Advanced maintenance and repair for offshore wind farms using fault prediction and condition monitoring techniques, funded by the European Commission.
[7] P. Caselitz and J. Giebhardt, "Condition monitoring and maintenance strategies for the next generation of large offshore wind turbines", ISET Offshore M&R Final Public Report.
[8] M. S. An, H. Y. Lim and D. S. Kang, "Implementation of Remote Condition Monitoring System of Offshore Wind Turbine Based on NI WSN", SERSC International Journal of Control and Automation, vol. 6, no. 2, **(2013)**, pp. 325-334.
[9] H. Polinder, H. Lendenmann, R. Chin and W. M. Arshad, "Fault tolerant generator systems for wind turbines", IEEE International Electric Machines and Drives Conference (IEMDC), **(2009)**, pp. 675 - 681.
[10] M. A. Parker, N. Chong and Ran Li, "Fault-tolerant control for a modular generator converter scheme for direct-drive wind turbines", IEEE Transactions on Industrial Electronics, vol. 58, no. 1, **(2011)**, pp. 305-315.
[11] F. Filippetti, G. Franceschini, C. Tassoni and P. Vas, "Recent developments of induction motor drives fault diagnosis using AI techniques", IEEE Transactions on Industrial Electronics, vol. 47, no. 5, **(2000)**, pp. 994-1004.
[12] B. Aravindh Kumar, G. Saranya, R. Selvakumar, R. Swetha Shree, M. Saranya and E. P. Sumesh, "Fault detection in Induction motor using WPT and Multiple SVM", SERSC International Journal of Control and Automation, vol. 3, no. 2, **(2010)**, pp. 9-20.
[13] J. Treetrong, "Fault Detection of Electric Motors Based on Frequency and Time-Frequency Analysis using Extended DFT", SERSC International Journal of Control and Automation, vol. 4, no. 1, **(2011)**, pp. 49-58.
[14] R. L. A. Ribeiro, C. B. Jacobina, E. R. C. Silva and A. M. N. Lima, "Fault detection of open-switch damage in voltage-fed PWM motor drive systems", IEEE Transactions Power Electronics, vol. 18, no. 2, **(2003)**, pp. 587-593.
[15] S. Heier and R. Waddington, "Grid Integration of Wind Energy Conversion Systems", John Wiley & Sons **(2006)**.
[16] P. C. Krause, "Analysis of Electric Machinery", McGraw-Hill, New York, **(1986)**.
[17] H. W. van der Broeck, H. C. Skudelny and G. V. Stanke, "Analysis and realization of a pulsewidth modulator based on voltage space vectors", IEEE Transactions on Industrial Applications, vol. 24, no. 1, **(1988)**, pp. 142-150.

[18] J. S. Ko, J. H. Lee and M. J. Youn, "Robust digital position control of brushless DC motor with adaptive load torque observer", IEE Electric Power Applications, vol. 141, no. 2, **(1994)**, pp. 63-70.
[19] Y. D. Landau, "Adaptive Control - The Model Reference Approach", Marcel Dekker, New York, **(1979)**.

Authors

Kyeong-Hwa Kim

Kyeong-Hwa Kim was born in Seoul, Korea, in 1969. He received the B.S. degree from Hanyang University, Seoul, Korea, and the M.S. and Ph.D. degrees from KAIST, Taejon, Korea, in 1991, 1993, and 1998, respectively, all in electrical engineering. From 1998 to 2000, he was a Research Engineer with Samsung Electronics Company, where he was engaged in research and development of AC machine drive systems. From 2000 to 2002, he was a Research Professor with KAIST. Since August 2002, he has been with Seoul National University of Science and Technology, where he is currently an Associate Professor. His current research interests are in the areas of AC machine drive, control, diagnosis, power electronics, renewable energy, and DSP-based control applications. Prof. Kim is a member of the Korean Institute of Power Electronics (KIPE).